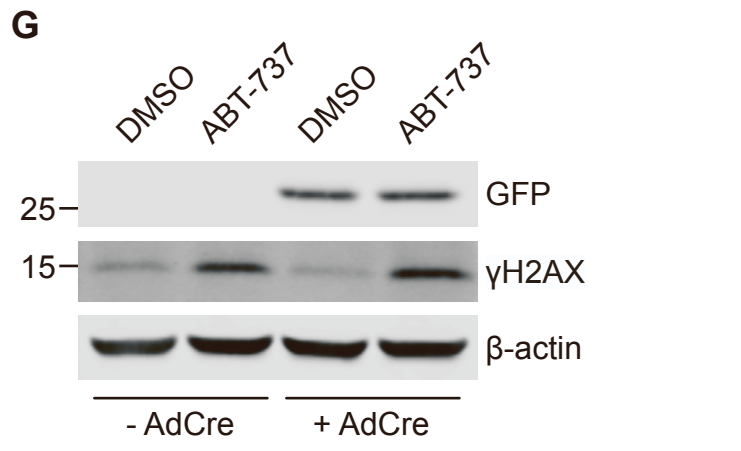
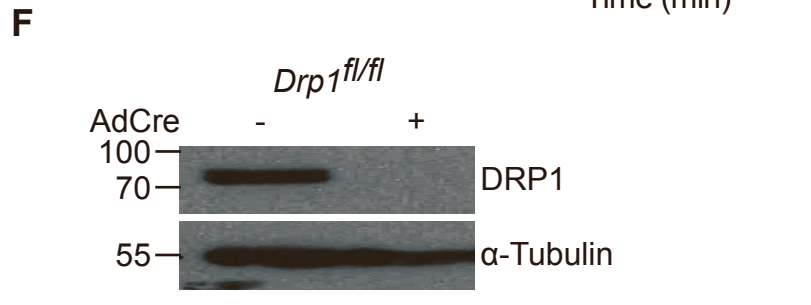
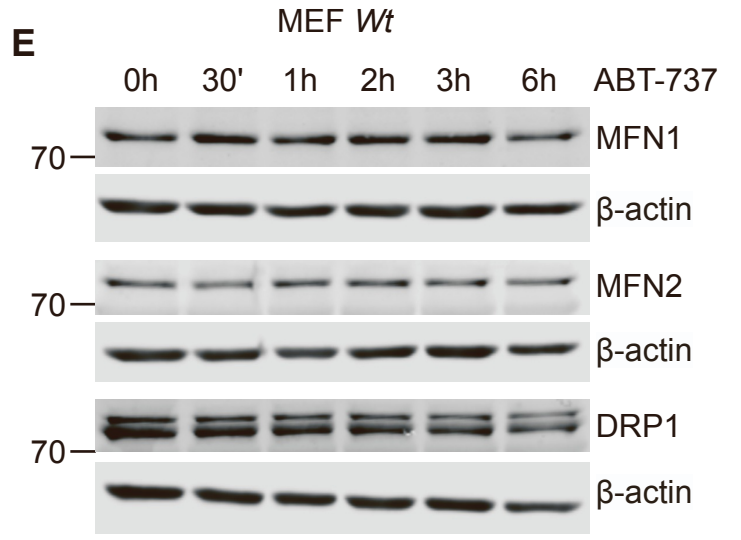
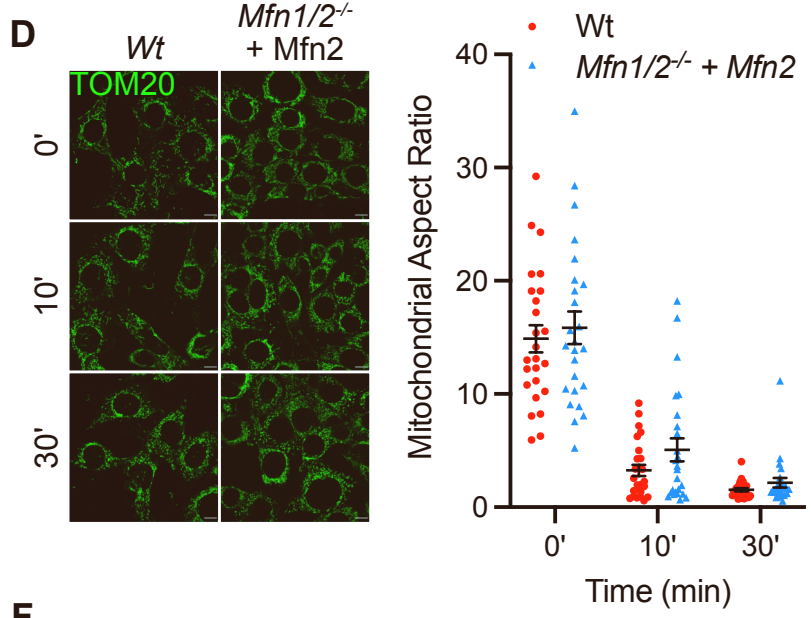
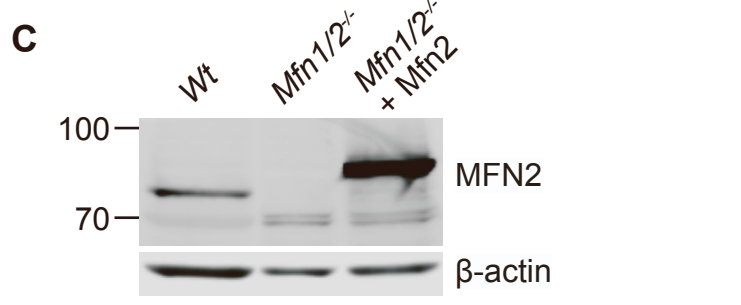
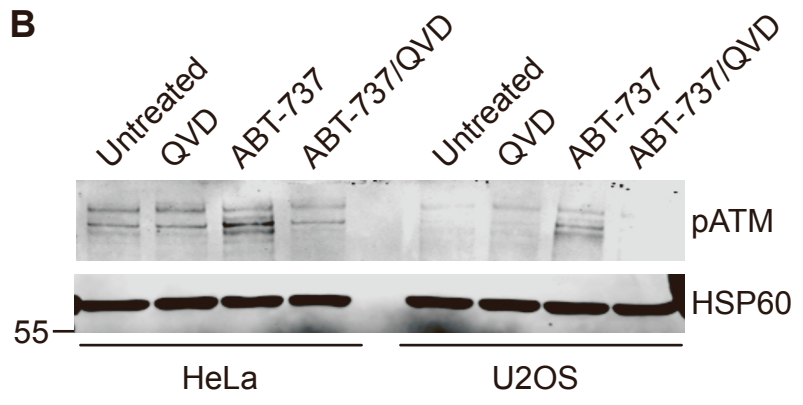
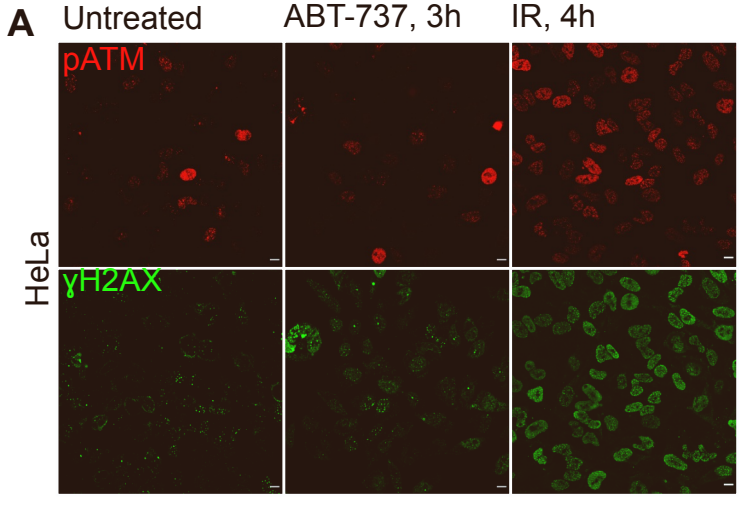


**Developmental Cell, Volume 57**

**Supplemental information**

**Mitochondrial dynamics regulate genome stability  
via control of caspase-dependent DNA damage**

**Kai Cao, Joel S. Riley, Rosalie Heilig, Alfredo E. Montes-Gómez, Esmee Vringer, Kevin Berthenet, Catherine Cloix, Yassmin Elmasry, David G. Spiller, Gabriel Ichim, Kirsteen J. Campbell, Andrew P. Gilmore, and Stephen W.G. Tait**



**Figure S1. Mitochondrial dynamics regulate DNA damage. Related to Figure 1**

- A) Airyscan images of HeLa cells treated with 10  $\mu$ M ABT-737 for 3 h, or 20 Gy irradiation for 4 h. Cells were immunostained with anti-pATM (red) or anti- $\gamma$ H2AX (green) antibody. Images representative of 3 independent experiments. Scale bar = 10  $\mu$ m
- B) Western blot of HeLa and U2OS cells treated with 10  $\mu$ M QVD, 10  $\mu$ M ABT-737 or a combination of both for 3 h. Blots were immunoblotted for pATM and HSP60 and a representative of 2 independent experiments.
- C) Western blot of *Wt*, *Mfn1/2<sup>-/-</sup>* and *Mfn1/2<sup>-/-</sup> + Mfn2* MEF immunoblotted for MFN2 and  $\beta$ -actin. Representative of 2 independent experiments.
- D) Airyscan images of *Wt* or *Mfn1/2<sup>-/-</sup> + Mfn2* MEF treated with 10  $\mu$ M CCCP for the indicated times and immunostained with anti-TOM20 antibody. Mitochondrial aspect ratio data is from 3 independent experiments. Data are expressed as mean  $\pm$  SEM.
- E) Western blot of *Wt* MEF treated with 10  $\mu$ M ABT-737 for 3 h, and immunoblotted for MFN1, MFN2, DRP1 and  $\beta$ -actin. Data are representative of 3 independent experiments.
- F) Western blot of *Drp1<sup>fl/fl</sup>* MEF with and without adenoviral Cre infection. Lysates immunoblotted for DRP1 and  $\alpha$ -tubulin.
- G) Western blot of loxP-STOP-loxP MEF infected or not with adenoviral Cre to induce YFP expression. Cells were treated with 10  $\mu$ M ABT-737 for 3 h and YFP expression analysed by GFP immunoblotting, DNA damage by  $\gamma$ H2AX and  $\beta$ -actin for loading control. Data is representative of 3 independent experiments.

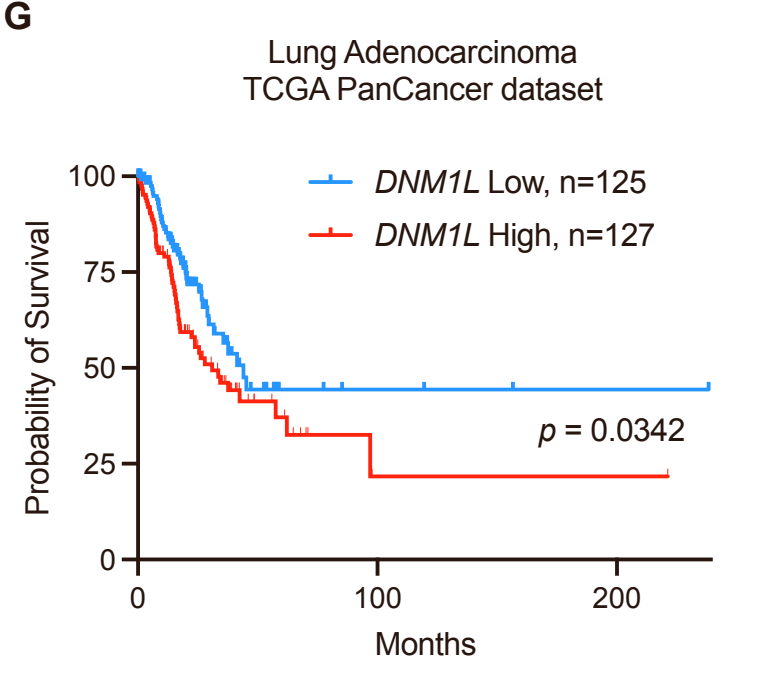
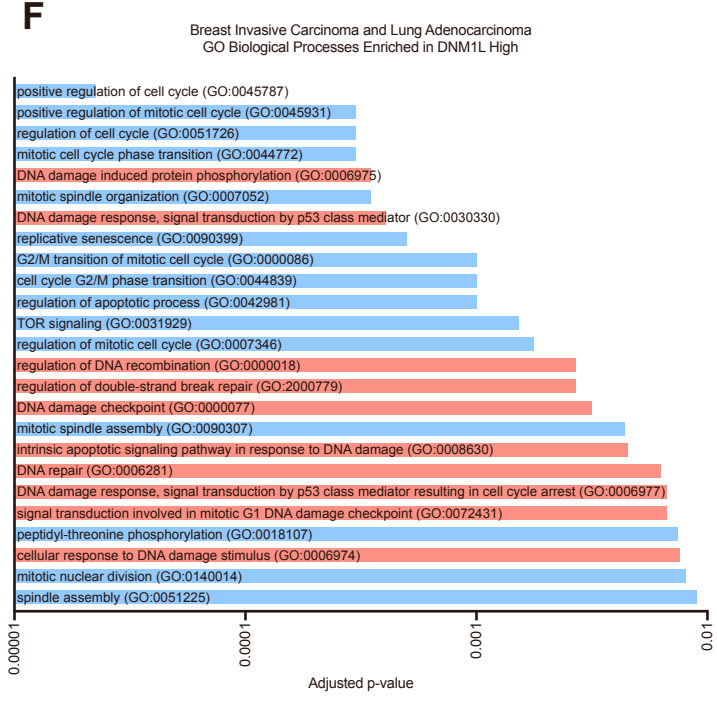
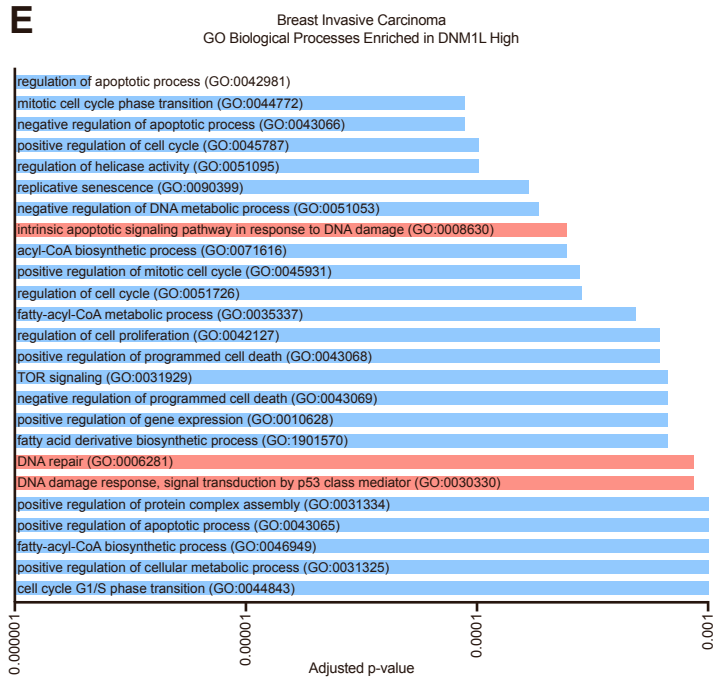
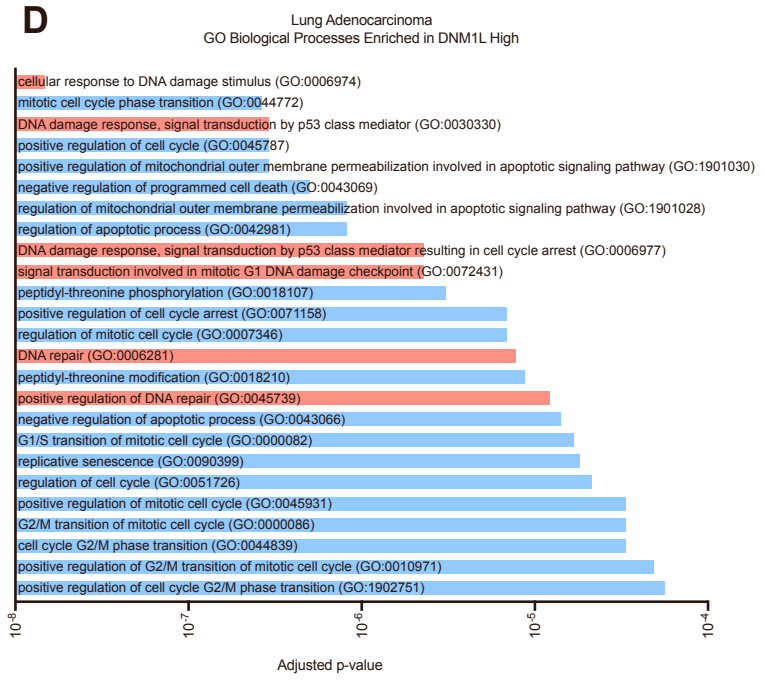
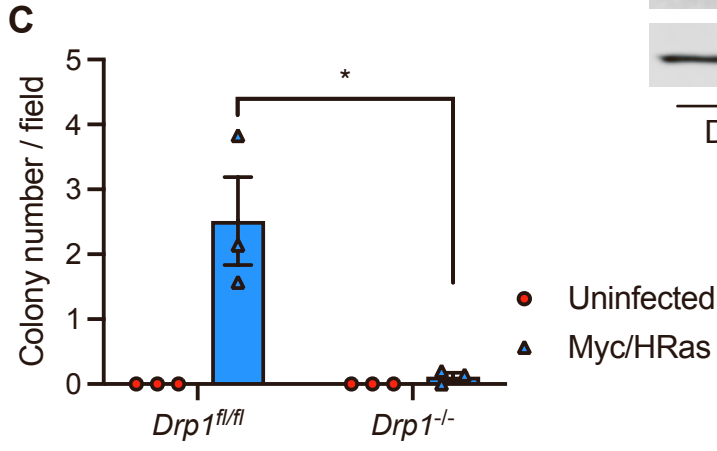
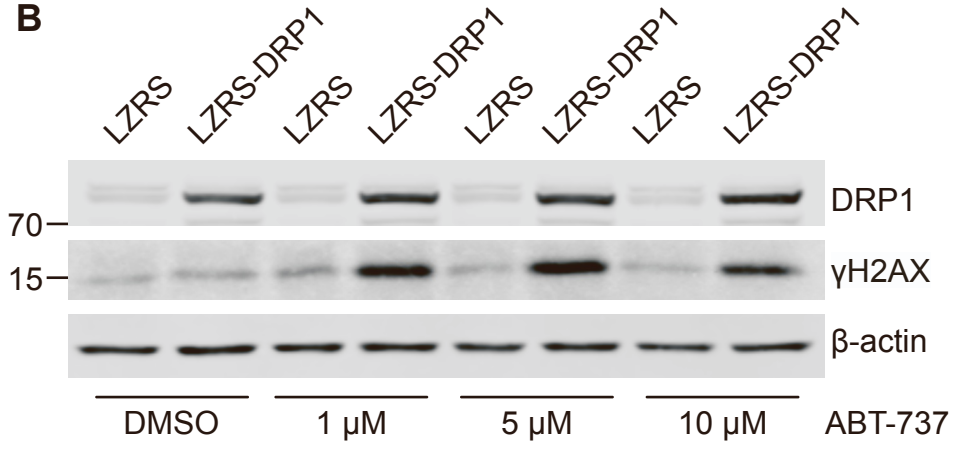
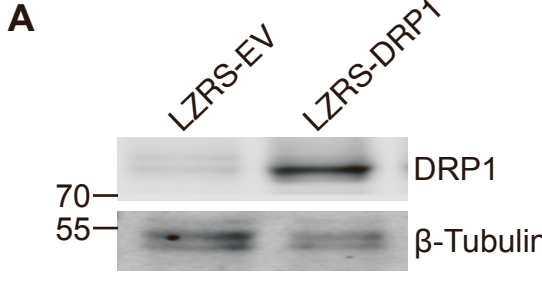


**Figure S2. Mitochondrial fission regulates DNA damage, transformation and cancer survival. Related to Figure 2**

- A) Western blot of MEF expressing LZRS empty control, or LZRS-DRP1. Lysates immunoblotted for DRP1 and  $\beta$ -tubulin.
- B) MEF stably overexpressing LZRS-DRP1 or LZRS empty vector were treated with the indicated dose of ABT-737 for 3 h and lysates immunoblotted for DRP1,  $\gamma$ H2AX and  $\beta$ -actin. Data are representative of 3 independent experiments.
- C) *Drp1<sup>fl/fl</sup>* and *Drp1<sup>-/-</sup>* MEF infected with viruses encoding Myc and HRas were cultured in soft agar and colony number quantified. Data are from 3 independent experiments, expressed as mean  $\pm$  SEM and analysed using student's t-test.
- D) Gene ontology (GO) biological processes significantly up-regulated in DNM1L high expressing lung adenocarcinoma samples. Bars in red represent GO biological processes related to DNA damage and are expressed as adjusted p-values.
- E) Gene ontology (GO) biological processes significantly up-regulated in DNM1L high expressing breast invasive carcinoma samples. Bars in red represent GO biological processes related to DNA damage and are expressed as adjusted p-values.
- F) Gene ontology (GO) biological processes significantly up-regulated in DNM1L high expressing lung adenocarcinoma and breast invasive carcinoma samples. Bars in red represent GO biological processes related to DNA damage and are expressed as adjusted p-values.
- G) Survival of lung adenocarcinoma patients. DNM1L Low refers to those patients in the lowest quartile of DNM1L mRNA expression, and DNM1L High refers to patients in the highest quartile. Significance is calculated by log-rank (Mantel-Cox) test.  
Statistics: \*  $p \leq 0.05$ , \*\*  $p \leq 0.01$ , \*\*\*  $p \leq 0.001$

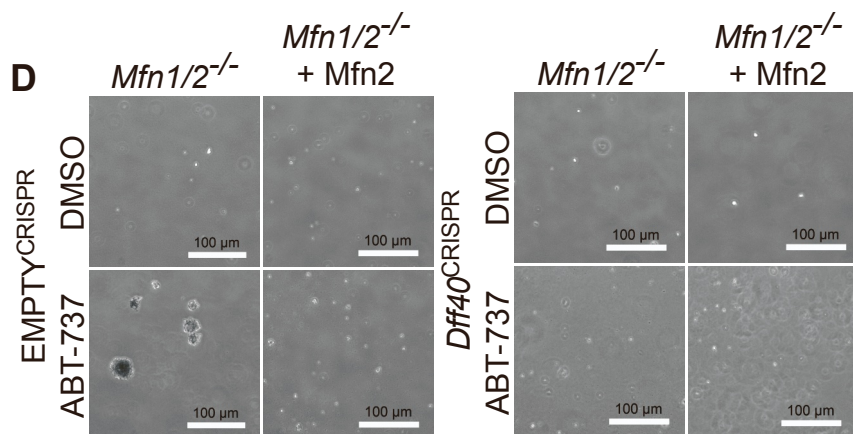
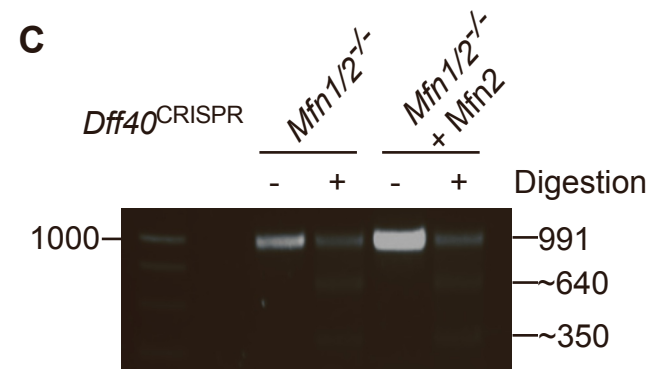
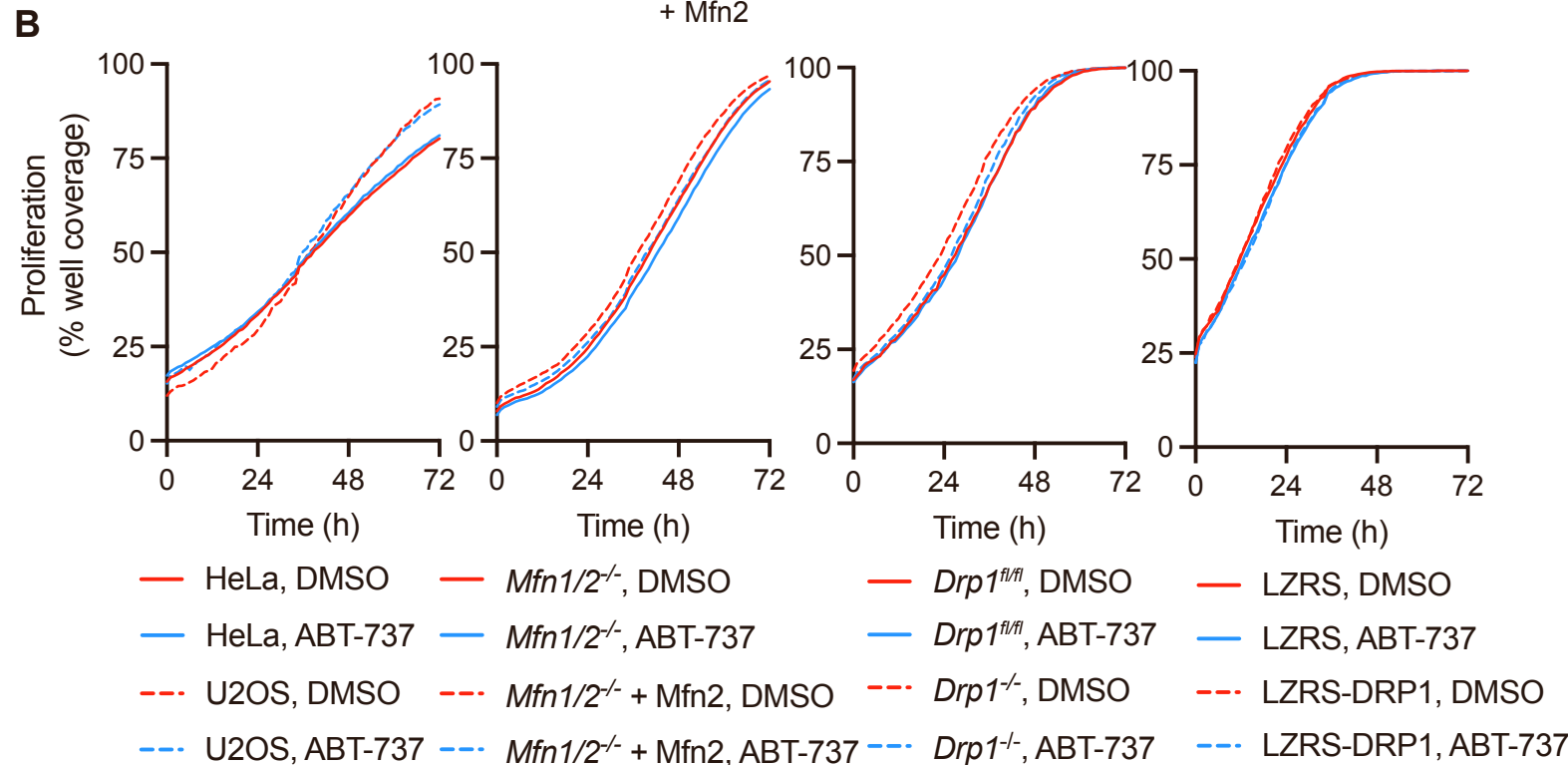
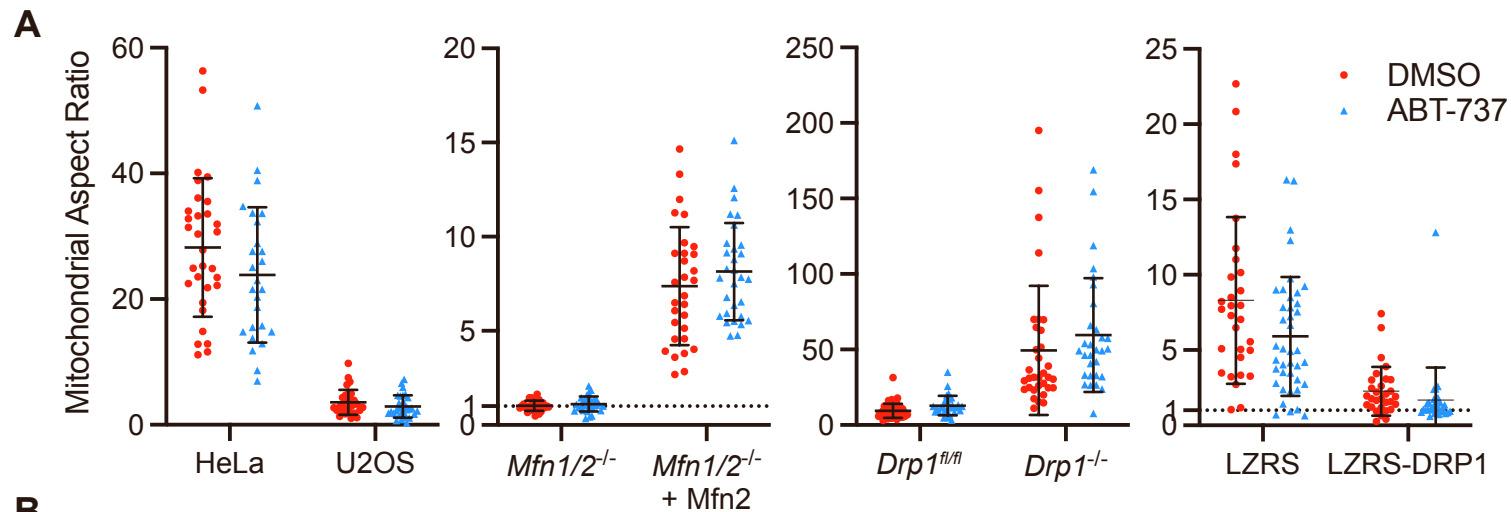


**Figure S3. Impact of mitochondrial fusion and fission machinery modulation on mitochondrial morphology, growth and CAD-dependent transformation. Related to Figure 4**

- A) Mitochondria aspect ratio of indicated cell lines treated with or without 10  $\mu$ M ABT-737 for 3 h. Cells were immunostained for TOM20 and imaged using Airyscan microscopy. Mitochondrial aspect ratio was calculated from 3 independent experiments and expressed as mean (SD).
- B) Proliferation of indicated cell lines treated with or without 10  $\mu$ M ABT-737 for 3h, after which time the media was changed to media not containing ABT-737. Cells were imaged for 72 h.
- C) T7 endonuclease I mismatch assay to assay for CAD/*Dff40* deletion.
- D) Representative images of anchorage-independent growth of *Mfn1/2*<sup>-/-</sup> and *Mfn1*<sup>-/-</sup> MEF with and without CRISPR-Cas9-mediated *Dff40* deletion. Cells were passaged twenty times in 10  $\mu$ M ABT-737. Scale bar = 100  $\mu$ m. Data are quantified in **Figure 2K**.

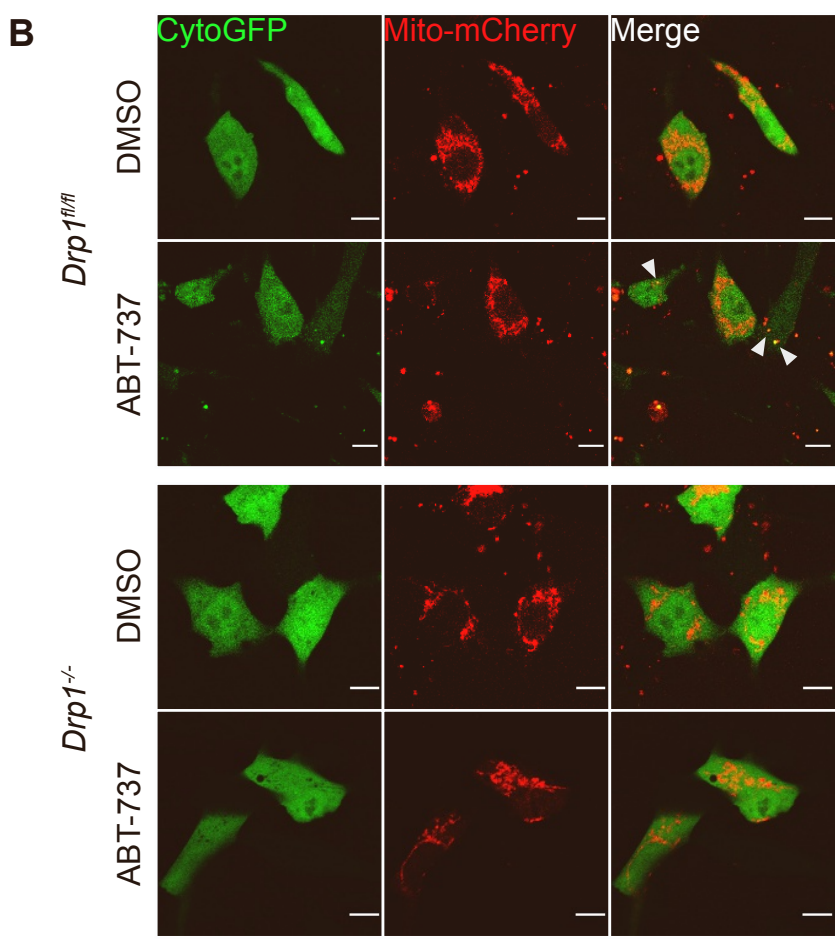
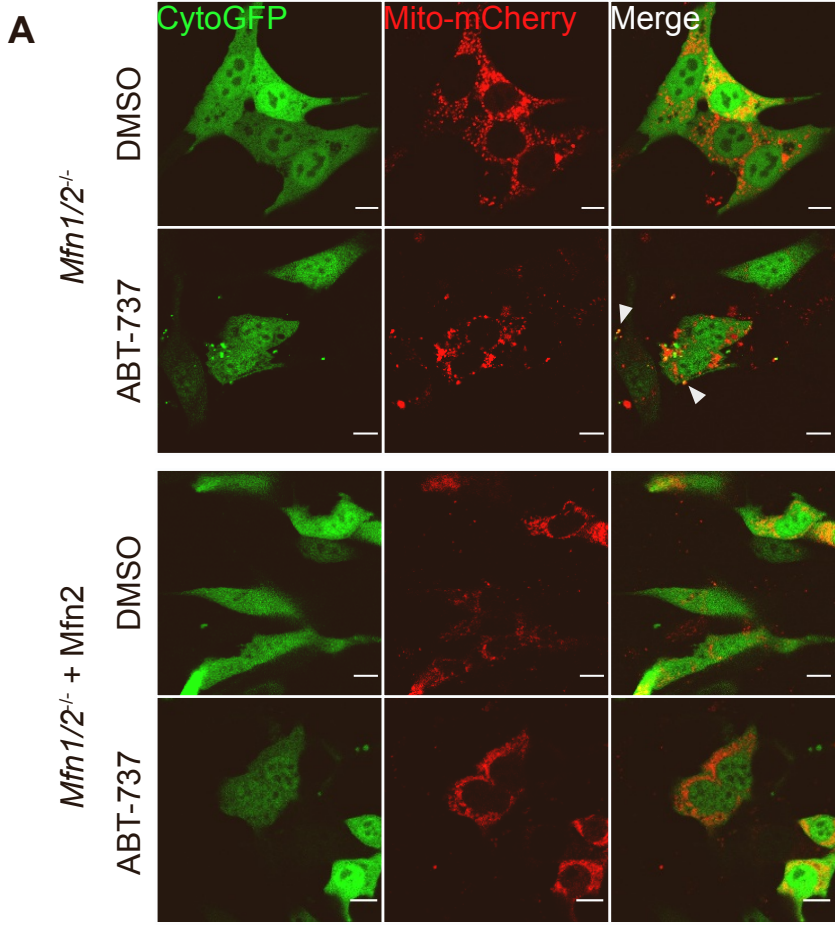




**Figure S4. Visualisation of minority MOMP in cells with modulated mitochondrial dynamics. Related to Figure 5.**

- A) Confocal images of *Mfn1/2<sup>-/-</sup>* and *Mfn1/2<sup>-/-</sup> + Mfn2* cells transiently expressing cytoGFP and mito-mCherry. Cells were treated with dimeriser and treated or not with 10  $\mu$ M ABT-737 for 3 h before fixation, imaging and quantification of minority MOMP. Images are quantified in **Figure 3E**.
- B) Confocal images of *Drp1<sup>fl/fl</sup>* and *Drp1<sup>-/-</sup>* cells transiently expressing cytoGFP and mito-mCherry. Cells were treated with dimeriser and treated or not with 10  $\mu$ M ABT-737 for 3 h before fixation, imaging and quantification of minority MOMP. Images are quantified in **Figure 3F**.

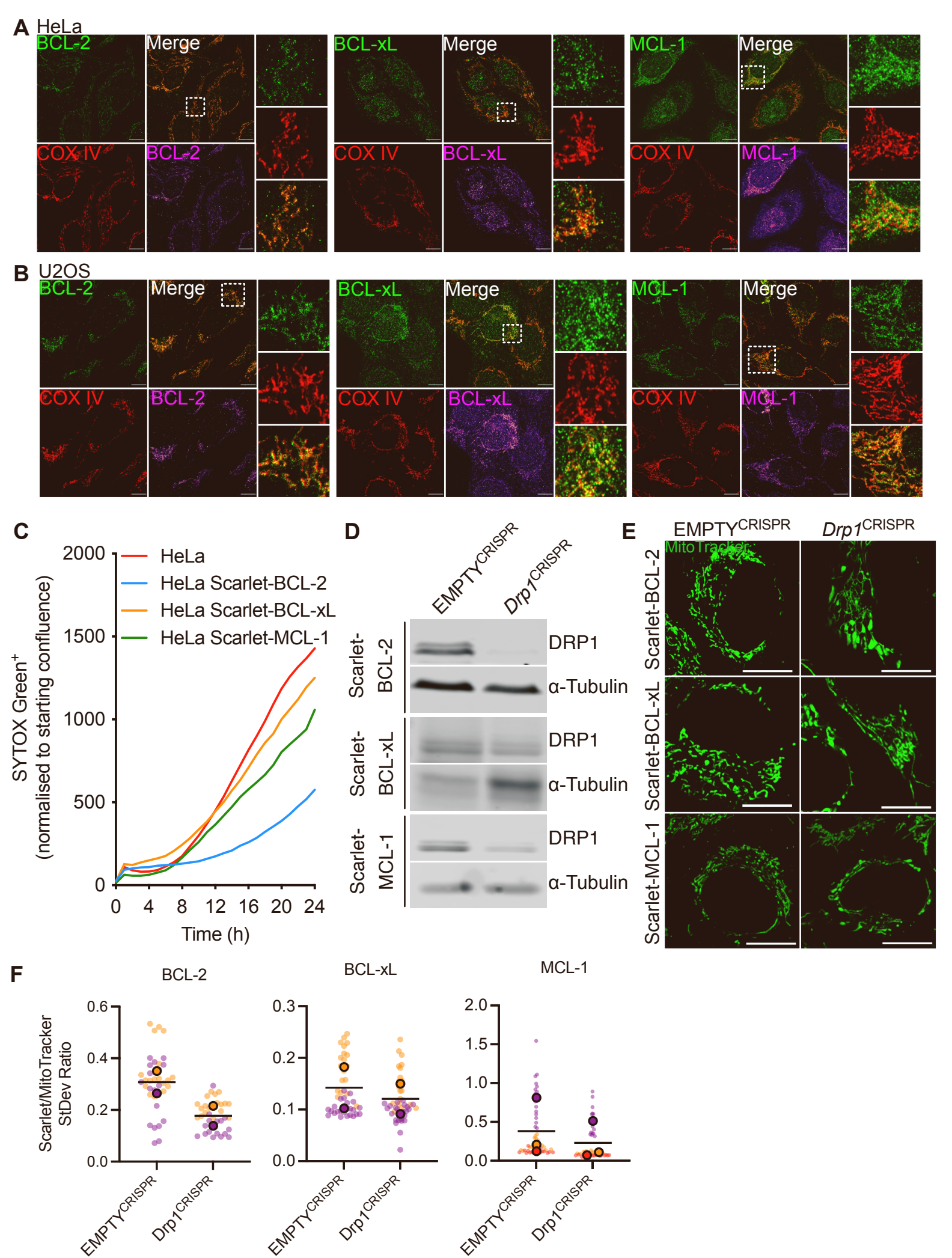


**Figure S5. Characterisation of BCL-2 family knockin cells. Related to Figure 6.**

- A) Airyscan images of HeLa cells immunostained for BCL-2, BCL-xL or MCL-1 (green) in combination with COX IV (red). Also shown are BCL-2, BCL-xL or MCL-1 images with a magenta LUT applied to visualise heterogeneity. Scale bar = 10  $\mu\text{m}$ . Data are representative of 3 independent experiments.
- B) Airyscan images of U2OS cells immunostained for BCL-2, BCL-xL or MCL-1 (green) in combination with COX IV (red). Also shown are BCL-2, BCL-xL or MCL-1 images with a magenta LUT applied to visualise heterogeneity. Scale bar = 10  $\mu\text{m}$ . Data are representative of 3 independent experiments.
- C) Live-cell IncuCyte analysis of HeLa and HeLa Scarlet-MCL-1 knockin cells treated with 10  $\mu\text{M}$  ABT-737 and 2  $\mu\text{M}$  S63845. Cells were incubated with SYTOX Green and SYTOX Green positivity was measured over time and normalised to starting confluency.
- D) Western blots of HeLa Scarlet-BCL-2, BCL-xL and MCL-1 knockin cells with CRISPR-Cas9-mediated DRP1 deletion. Lysates immunoblotted for DRP1 and  $\alpha$ -tubulin as a loading control.
- E) Representative Airyscan images of mitochondrial structure in HeLa Scarlet-BCL-2, BCL-xL and MCL-1 knockin cells with CRISPR-Cas9-mediated DRP1 deletion. Scale bar = 10  $\mu\text{m}$ . Data are representative of at least 2 independent experiments.
- F) Quantification of standard deviation of Scarlet to MitoTracker signal in HeLa Scarlet BCL-2, BCL-xL and MCL-1 cells, with or without CRISPR-Cas9-mediated DRP1 deletion. Data are expressed as borderless points for individual cells and points with borders represent summary data for  $n = 2$  biological replicates for BCL-2 and BCL-xL, and  $n = 3$  for MCL-1. The line represents the mean.

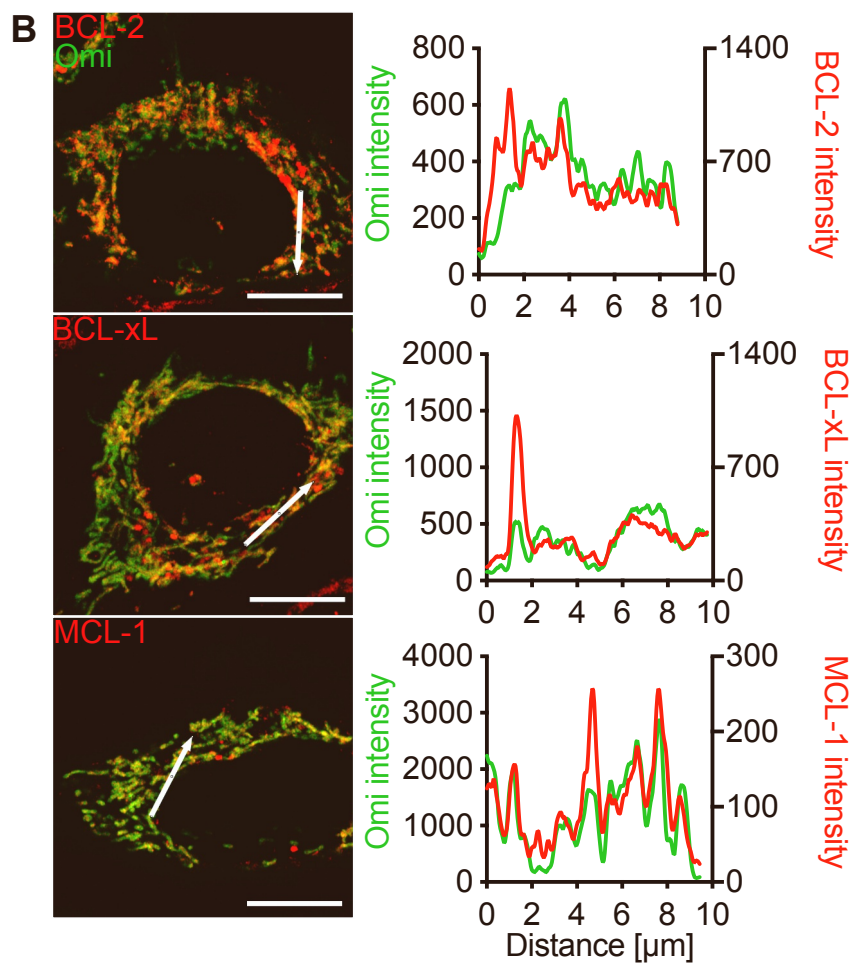
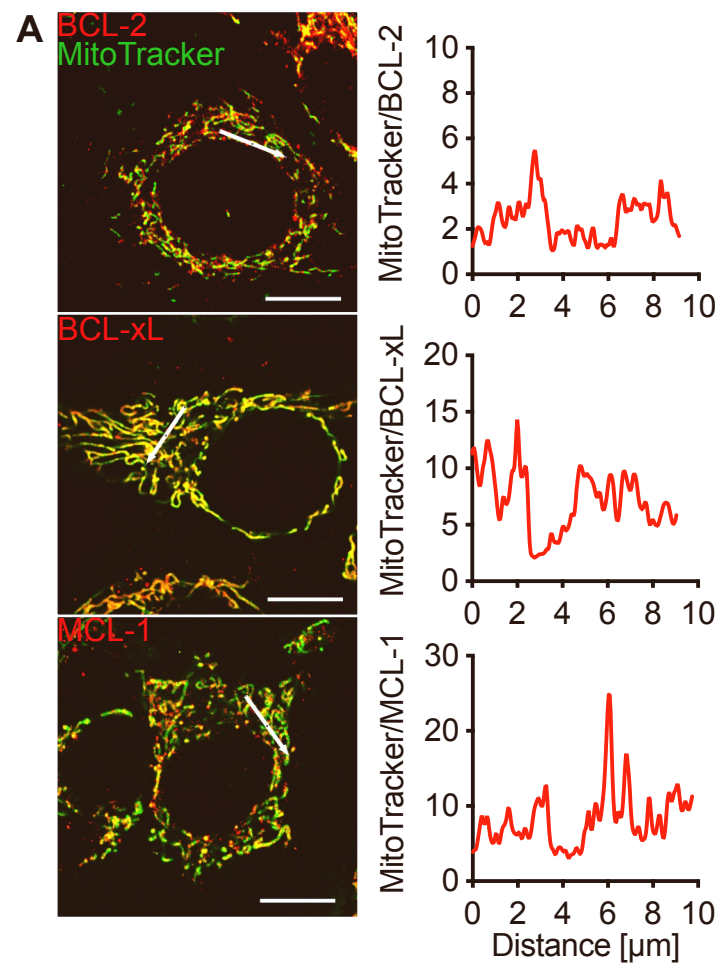


**Figure S6. Mitochondrial localisation of BCL2-family knockins. Related to Figure 5.**

- A) Airyscan images of HeLa Scarlet-BCL-2, BCL-xL and MCL-1 knockin cells and MitoTracker. Line scans show ratio of MitoTracker to Scarlet-BCL-2. Scale bar = 10  $\mu$ m. Data representative of 3 independent experiments.
- B) Airyscan images of HeLa Scarlet-BCL-2, BCL-xL and MCL-1 knockin cells and Omi-GFP. Line scans show ratio of Omi-GFP intensity (green) and Scarlet-BCL-2 intensity (red). Scale bar = 10  $\mu$ m. Data representative of 3 independent experiments.

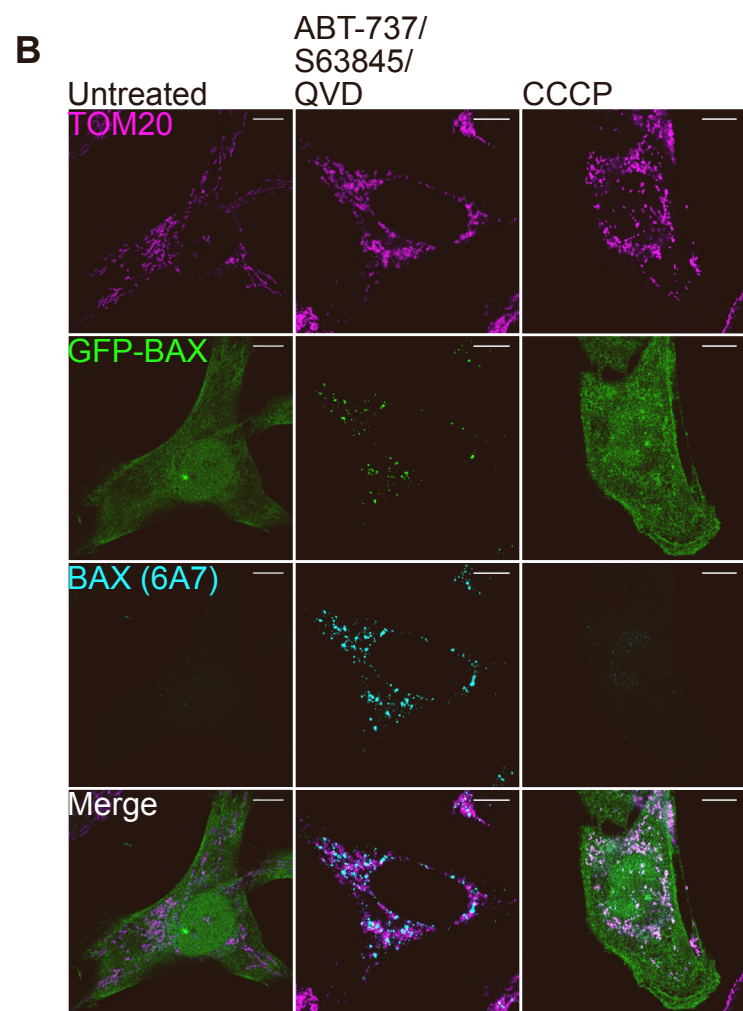
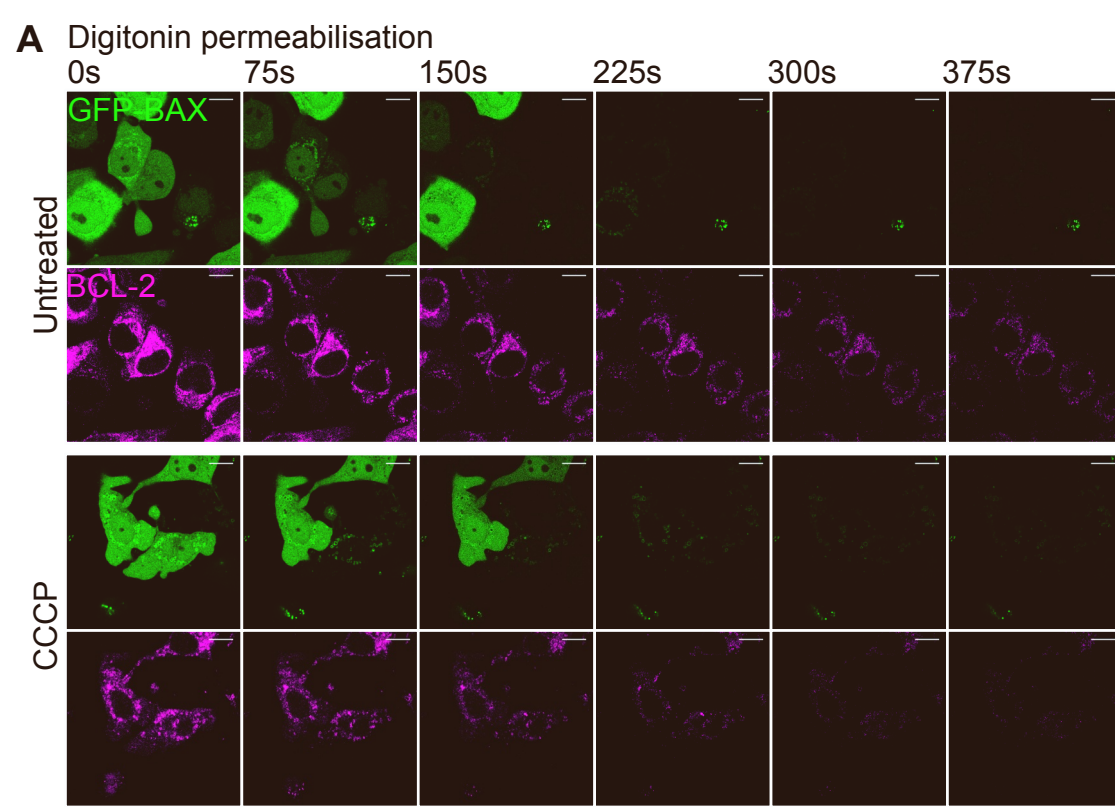


**Figure S7. Mitochondrial dysfunction causes BAX accumulation on the mitochondrial outer membrane, but not BAX pore formation. Related to Figure 6.**

- A) Images of HeLa Scarlet-BCL-2 knockin (magenta) cells stably overexpressing GFP-BAX (green) treated 10  $\mu$ M CCCP for 30 min before digitonin permeabilisation. Scale bar = 10  $\mu$ m. See also **Videos S4, S5**.
- B) Airyscan images of fixed HeLa cells stably overexpressing GFP-BAX (green) and treated with 10  $\mu$ M CCCP or 10  $\mu$ M ABT-737, 2  $\mu$ M S63845 and 10  $\mu$ M QVD for 3 h. Cells were immunostained with anti-TOM20 (magenta) and anti-BAX 6A7 (cyan). Scale bar = 10  $\mu$ m. Images representative of 3 independent experiments.